Attempt of applying the interacting-boson-fermion model to the superdeformed bands of ^{191,193}Hg

H. C. Chiang and S. T. Hsieh
Tsing Hua University, Hsinchu, Taiwan, Republic of China
(Received 9 July 1998; published 9 September 1999)

Energy levels, dynamic moments of inertia of the superdeformed bands of ^{191,193}Hg are studied by incorporating fermion degrees of freedom with the superdeformed interacting boson model. Except for the cases with band crossing, it is found that the single-fermion orbital dominance is sufficient for describing most of the superdeformed bands. The energy levels can be reproduced quite well. The dynamic moments of inertia can be reproduced reasonably well for most of the bands. However, the staggering of the moment of inertia observed in some superdeformed bands cannot be reproduced in the model. The general features of the wave functions are discussed. [S0556-2813(99)04509-4]

PACS number(s): 21.60.Fw, 21.10.Re, 27.80.+w

I. INTRODUCTION

In recent years, many superdeformed bands have been found for even-odd as well as even-even nuclei. In a given mass region, the superdeformed bands usually show similar energy band structures and moments of inertia. It is generally believed that these superdeformed bands can be described by the couplings between the fermion single-particle degrees of freedom and a highly deformed core. Therefore, for the mass region $A=190$, the high-N intruder orbitals such as $h_{11/2}$, $i_{13/2}$, and $j_{15/2}$ are expected to be important for describing the configurations of the superdeformed states.

The interacting boson model (IBA) [1–3] has been applied extensively to study collective nuclear states which include the cases of highly deformed ones. The IBA model was extended to describe even-odd nuclei by coupling a single fermion to the even-even core [4,5]. The model which is usually called interacting-boson-fermion approximation (IBFA) has been applied successfully in correlating the nuclear properties of the normal collective even-odd nuclei [6–10].

Based on the dominance of the $J^{\pi}=0^{+}$ and 2^{+} nuclear pairs in the Nilsson wave functions, Otsuka and Honma proposed an algebraic superdeformed interacting boson model [11]. In this model the inert core is smaller as compared with the normal interacting-boson model and the number of valence bosons is increased considerably since more active major shells are considered. The model with the restrictions to specific dynamic symmetries was applied to analyze the superdeformed states of even-even nuclei [12,13]. In this work, we attempt to combine the single-fermion degrees of freedom with the superdeformed interacting-boson model to make a detailed phenomenological calculation on the energy levels and dynamic moment of inertia of the superdeformed bands of the even-odd Hg isotopes.

II. MODEL

In our working model ^{191,193}Hg isotopes are considered as the coupling system of even-even cores of ^{190,192}Hg with a fermion. In the superdeformed interacting boson model a smaller inert core is adopted. For the mass region we are considering, ^{132}Sn is considered as an appropriate core. The nucleon pairs outside the core are imitated by active bosons. Since we are working in a well deformed region, the distinction between the proton- and neutron-boson can be ignored. Therefore, ^{190,192}Hg can be considered to have 29 and 30 interacting bosons, respectively (including s and d bosons) outside the ^{132}Sn core. The ^{191,193}Hg isotopes are then considered to have 29, 30 interacting bosons plus one fermion. The possible fermion single-fermion orbitals are the $1h_{11/2}$, $1i_{13/2}$, and $1j_{15/2}$ orbitals. Previous analyses on the superdeformed bands of ^{191,193}Hg suggest that most of the bands are dominated by one of the above single-fermion orbitals [14–19]. Therefore, in calculating a specific band, we include the corresponding dominant fermion orbital in the model space. To be more specific, $h_{11/2}$ orbital is included in band 1 and band 2a of ^{193}Hg; $i_{13/2}$ orbital is included in bands 2 and 3 of ^{191}Hg, and in bands 2b and 3 of ^{193}Hg; $j_{15/2}$ orbital is included in bands 1 and 4 of ^{191}Hg, and in bands 4 and 5 of ^{193}Hg. The model spaces as described are too big for practical calculation. Therefore, we tried to make a reasonable truncation on the boson model space. Similar to the truncation scheme usually used in the shell model, we restricted the number of bosons in the higher single-boson energy orbital. Therefore, we restrict the number of d bosons n_d by $n_d \leqslant L/2+10$ where L means the total boson angular momentum. With this truncation the dimension of the model space of the energy matrix for a specific value of spin can be reduced to about 300 which is feasible for practical calculation. For the Hamiltonian we adopted the usual form used in the IBFA calculation:

$$H=H_B+H_F+H_{BF}.$$

Here H_B means the Hamiltonian of interacting bosons which takes the form [20]

$$H_B=\varepsilon_d n_d+c_0 p^{\dagger}p+c_1\frac{L\cdot L}{1+fL\cdot L}+c_2 Q_B\cdot Q_B,$$

where n_d means d-boson number operator and $p^{\dagger}p$, $L\cdot L$, and $Q\cdot Q$ are the boson pairing, angular momentum, and quadrupole interactions, respectively. A $fL\cdot L$ term is in-

cluded in the denominator of the angular momentum interaction to account for the antipairing effects for the high spin states [21]. The fermion Hamiltonian H_F includes only single-fermion energies. Since we include only the dominant single-fermion orbital, this term appears as a constant for each band. Therefore, it can be ignored as far as excitation energies are calculated. The boson-fermion Hamiltonian H_{BF} includes the boson-fermion quadrupole interaction and the exchange force term:

$$H_{BF}=KQ_B\cdot Q_F+\sum_{k,j_1,j_2}:\Lambda^k_{j_1j_2}[(a^\dagger_{j_1}\times\tilde{d})^{(k)}\times(d^\dagger\times\tilde{a}_{j_2})^{(k)}]^{(0)}:,$$

where Q_B is the boson quadrupole operator

$$Q_B=(s^\dagger\times\tilde{d}+d^\dagger\times\tilde{s})-\frac{\sqrt{7}}{2}(d^\dagger\times\tilde{d})^{(2)}$$

and Q_F is the fermion quadrupole operator

$$Q_F=\sum_{j_1j_2}q_{j_1j_2}(a^\dagger_{j_1}\times\tilde{a}_{j_2})^{(2)}$$

and $q_{j_1j_2}=\sqrt{5}\langle j_1\|Y^{(2)}\|j_2\rangle$.

In this work, we choose $j_1=j_2=j$ where j is the angular momentum quantum number for the dominant single-fermion orbital. The second term in H_{BF} is the exchange force term and the $::$ symbol means normal ordering of the operators in between, and

$$\Lambda^k_{jj}=-2\Lambda\left(\frac{5}{2k+1}\right)^{1/2}\langle j\|Y^2\|k\rangle\langle k\|Y^{(2)}\|j\rangle.$$

The monopole interaction term which is adopted in other calculations of similar model is omitted. This is because this term is proportional to n_d and can be absorbed in $\varepsilon_d n_d$ term by renormalizing ε_d. Since quite numerous active bosons are included in the model space, an efficient way of calculating the d-boson coefficient of parentage (cfp) is needed. The cfp's which are needed in constructing the many boson wave functions are calculated by using a group theoretical method proposed by Sun *et al.* [23]. The chosen Hamiltonian is then used to construct the energy matrices in the adopted model space. The interaction parameters in the Hamiltonian are determined by least-squares fittings with the energy levels of the superdeformed bands. In the fittings, as a first trial, we included all interaction terms and all of the interaction parameters are varied to improve the fittings. However, in the fitting procedures if a interaction term is proved to be quite insensitive to the fittings, the corresponding interaction parameter will be omitted to reduce the number of parameters.

TABLE I. Best fitted interaction parameters in MeV for ^{191,193}Hg in the IBFA model.

		ε_d	c_1	K	f
^{191}Hg	Band 1	0.1021	0.0050	−0.0161	3.30×10^{-5}
	Band 2	0.0837	0.0050	−0.0138	3.55×10^{-5}
	Band 3	0.0906	0.0049	−0.0130	3.97×10^{-5}
	Band 4	0.0173	0.0057	−0.0158	7.35×10^{-5}
^{193}Hg	Band 1	0.0712	0.0049	−0.0192	6.32×10^{-5}
	Band 2a	0.0719	0.0050	−0.0161	3.75×10^{-5}
	Band 2b	0.1045	0.0050	−0.0109	4.15×10^{-5}
	Band 3	0.1108	0.0050	−0.0091	4.10×10^{-5}
	Band 4	0.0494	0.0052	−0.0143	4.94×10^{-5}
	Band 5	0.1042	0.0052	−0.0093	2.55×10^{-5}

III. RESULTS

A. Interaction parameters

In searching for the interaction parameters by least-squares fittings, a set of the initial values is needed. Therefore, we first turned off the single-fermion energy and boson-fermion interaction in the Hamiltonian. The interaction parameters in H_B are determined by least-squares fittings to the energy levels of the superdeformed bands of ^{190,192}Hg. The resulting values are then used as the initial values in the calculation of the superdeformed bands of ^{191,193}Hg. In the calculation on ^{190,192}Hg, it was found that the boson pairing and quadrupole interaction terms are not sensitive to the least-squares fittings. Therefore, these terms are omitted from H_B. The absence of these terms corresponds to the SU(5) limit in the interaction boson model [20]. This is also consistent with the result of Ref. [13] which calculated the superdeformed bands of even-even nuclei based on an interacting boson model in the SU(5) limit including g boson. By choosing $a_0=a_2=0$, the number of boson interaction parameters is reduced from 5 to 3. This greatly facilitates the least-squares fitting calculations. In the calculation on the even-odd Hg isotopes the boson-fermion interaction parameters K and Λ are also included in the least-squares fittings. Again, as a first trial, all interaction terms are treated on an equal footing. However, it was found that the quality of fittings to the energy levels of the superdeformed band does not depend on the values of Λ. Therefore, we omit this term and ended with only four parameters in the fittings. The best fitted interaction parameters are summarized in Table I. It can be seen from the table that the values of c_1 and K are similar for all superdeformed bands. The values of the s-d boson energy gap (ε_d) are different for different bands. However, they are all much smaller than the corresponding values for the normal boson cases [10]. It is well known in IBA calculations that the value of ε_d is getting smaller when the deformation is increased. The smaller values of ε_d found in this work are consistent with the general tendency. This also, in turn, suggests that both bands 4 of ^{191,193}Hg are more deformed than the other bands. The values of f are all quite small. This term is needed to fit the energy states for very high spins. Also, it has the effect to suppress the calculated dynamic moments of inertia (J_2) at high spin regions.

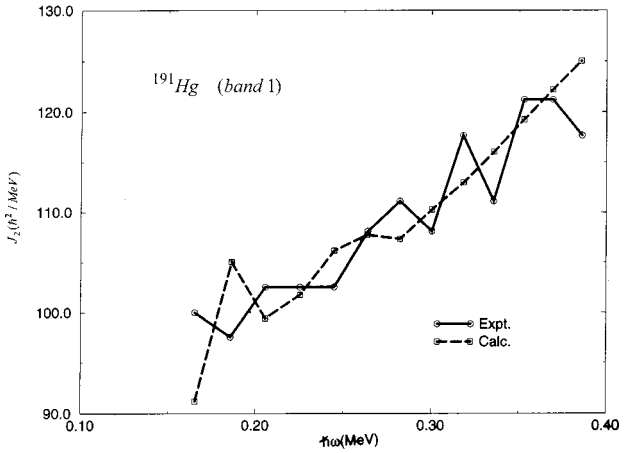

FIG. 1. Calculated and experimental J_2 values for superdeformed band 1 of ^{191}Hg. The dynamic moment of inertia is defined as $4[E_r(I+2)-E_r(I)]^{-1}$ where $E_r(I)$ means the transition energy of angular momentum I state in MeV. The rotational energy $\hbar\omega$ is defined as $\frac{1}{4}[E_r(I)+E_r(I+2)]$. The experimental data are adopted from Refs. [19] and [22].

B. Dynamic moment of inertia

The calculated energy levels are very close to the experimental data. For ^{191}Hg the overall root-mean-square (rms) deviations for all superdeformed band are around 1 keV or smaller. For ^{193}Hg the rms's are around 2 keV. Even for the low-lying states in the superdeformed bands the level spacing is around 0.3 MeV. Therefore, the usual plot which compares the calculated and experimental energy levels is not very illuminating. We present instead, the comparison of the calculated and experimental dynamic moments of inertia (J_2) which are very sensitive to the theory-experimental discrepancies. The calculated and experimental J_2 values of ^{191}Hg are shown in Figs. 1–4. From the figures we can see that the general tendency of the increase of J_2 versus the variation of $\hbar\omega$ can be reproduced. The theory-experiment agreements are very good if the experimental values of J_2 vary smoothly with rotational energies. If the experimental values of J_2 vary in zigzag forms, the calculated and experimental values agree with each other in the sense of average values. At the upper end of $\hbar\omega$ the experimental values of J_2 show some tendency of going down (bands 1,2). This trend cannot be reproduced in the calculation. It will be interesting to see whether this trend of downturn of the experimental values of J_2 will continue for higher rotational energies. The calculated and experimental values of J_2 of ^{193}Hg are shown in Figs. 5–10. The quality of agreement is similar to that of ^{191}Hg. Again, in the region that the experimental data vary quickly the calculated values can fit the data only in the sense of average values. For bands 1, 2b, 3, and 4, the calculated J_2 values are higher than the experimental data at the upper end of rotational energy. Of particular interest are the J_2 values of band 1 at high rotational energies. The experimental data show a rather flat behavior. On the other hand, the calculated values increase smoothly versus the increase of the rotational energy. The failure in reproducing these J_2

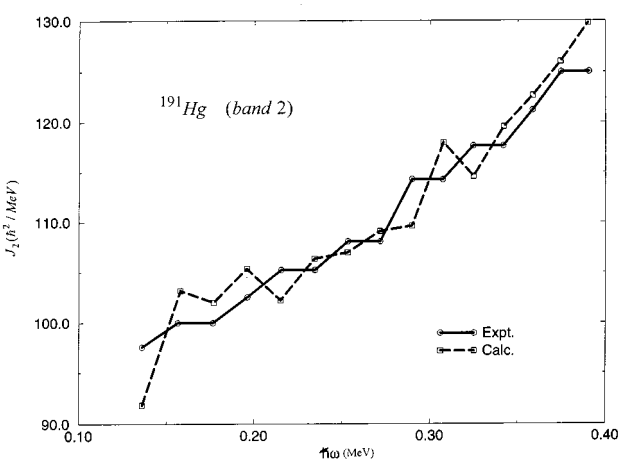

FIG. 2. Calculated and experimental J_2 values for superdeformed band 2 of ^{191}Hg. The experimental data are adopted from Refs. [19] and [22].

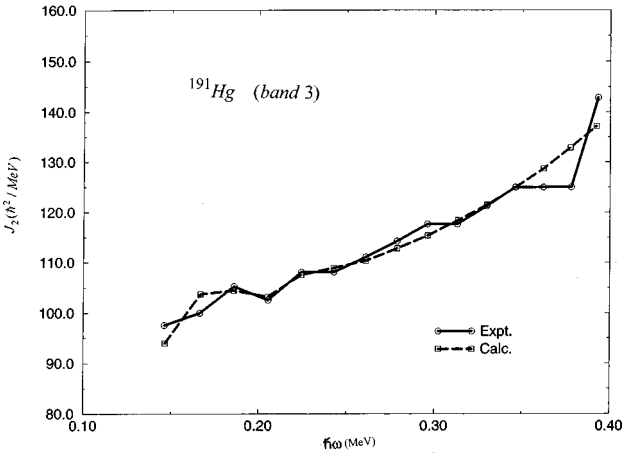

FIG. 3. Calculated and experimental J_2 values for superdeformed band 3 of ^{191}Hg. The experimental data are adopted from Refs. [19] and [22].

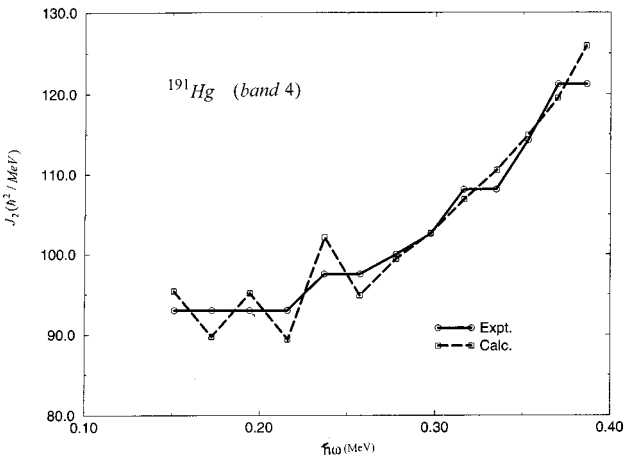

FIG. 4. Calculated and experimental J_2 values for superdeformed band 4 of ^{191}Hg. The experimental data are adopted from Refs. [19] and [22].

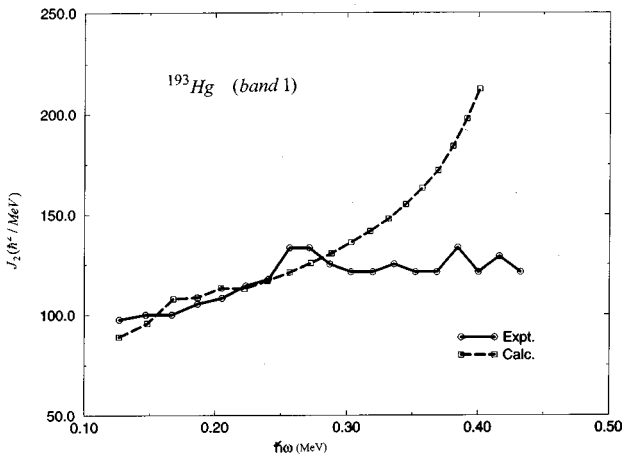

FIG. 5. Calculated and experimental J_2 values for superdeformed band 1 of ^{193}Hg. The experimental data are adopted from Ref. [18].

values after $\hbar\omega=0.27$ MeV seems to be consistent with the conjecture of orbital crossing at this point [16,22]. However, the calculated J_2 values of band 4 up to $\hbar\omega=0.4$ MeV fit the experimental data quite well. If band 4 also has an orbital crossing as conjectured, it seems the crossing energy will be much higher than that for band 1.

C. Wave functions

The basis states used in this work are the boson basis states coupled with the single-particle fermion basis states. For the boson basis states the following group chain is selected:

$$U(6)\supset U(5)\supset O(5)\supset O(3).$$

Therefore, the basis states are characterized by the form $|n_s n_d v n_\Delta L\rangle$ where n_s and n_d are the number of s and d bosons, v means d-boson seniority, n_Δ counts d-boson triplets coupled to zero angular momentum, and L means boson total angular momentum. The fermion single-particle wave-

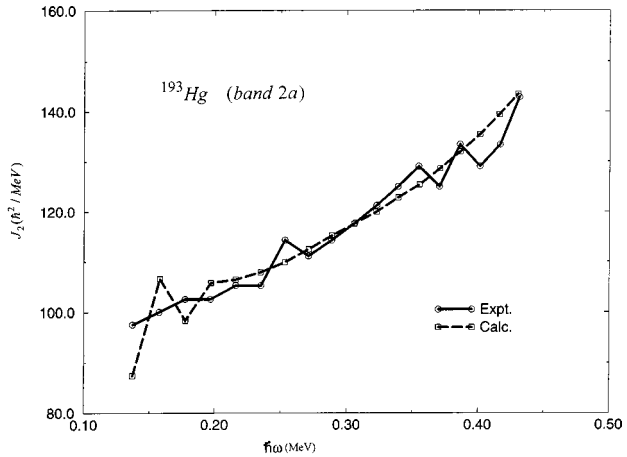

FIG. 6. Calculated and experimental J_2 values for superdeformed band 2a of ^{193}Hg. The experimental data are adopted from Ref. [18].

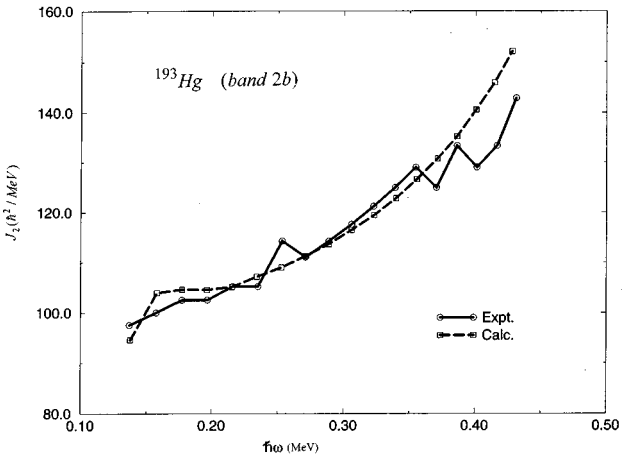

FIG. 7. Calculated and experimental J_2 values for superdeformed band 2b of ^{193}Hg. The experimental data are adopted from Ref. [19].

function $|j\rangle$ is simply characterized by its orbital angular momentum. For a specific value of boson-fermion total angular momentum J the dimension of the truncated model space is still quite large. Usually it is over 300 for the J values between $\frac{35}{2}$ and $\frac{87}{2}$. For the J values outside this range the dimension decreases. It is around 200 for $J=\frac{19}{2}$ and 150 for $J=\frac{99}{2}$. An analysis of the energy eigenfunctions indicates that the intensity distributions are in general rather dispersive, although only about one fifth of the basis states make significant contributions. However, we can still find some interesting features for those important basis states: (i) The boson angular momentum L and fermion angular momentum j satisfy $L+j=J$. (ii) Low n_d states are in general more important than the higher n_d states. This low n_d dominance becomes more prominent as J increases. This also justifies our truncation scheme in the model space. (iii) For a given value of n_d, only those states with $v=n_d$; $v=n_d-2$ and $v=n_d-4$ are important. (iv) Most of the important states have $n_\Delta=0$. The rest of the few such states have $n_\Delta=1$. From these features, it seems that the bosons and the fermion

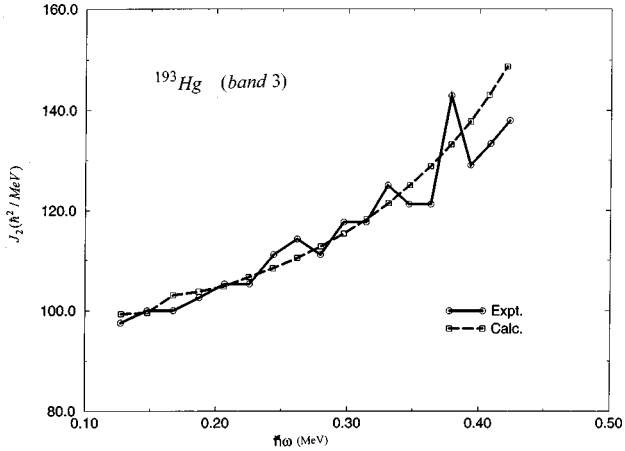

FIG. 8. Calculated and experimental J_2 values for superdeformed band 3 of ^{193}Hg. The experimental data are adopted from Ref. [18].

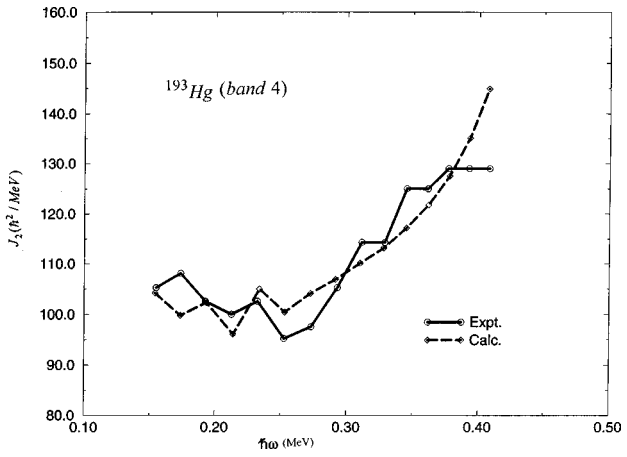

FIG. 9. Calculated and experimental J_2 values for superdeformed band 4 of ^{193}Hg. The experimental data are adopted from Ref. [18].

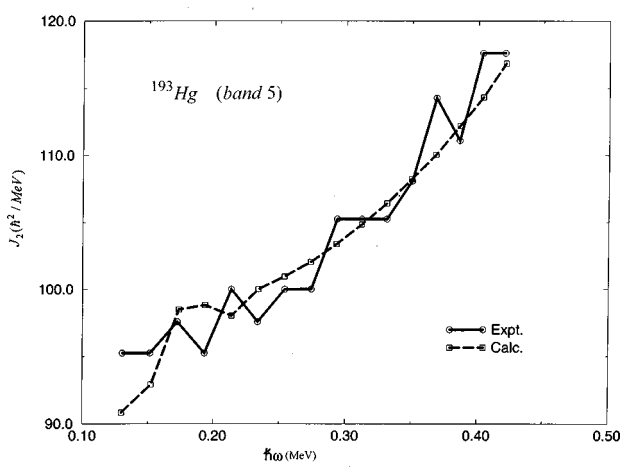

FIG. 10. Calculated and experimental J_2 values for superdeformed band 5 of ^{193}Hg. The experimental data are adopted from Ref. [18].

tend to assume a most economic coupling to reach the high spin. This is because it has the effect to reduce the needed number of d bosons and in turn, reduces the energy eigenvalue. This is consistent with the tendency that stability selects low energy configurations. The low value dominance of n_Δ is also reasonable. A higher value of n_Δ means more d-bosons coupled to zero angular momentum. This has the effect to restore the nucleus to a more spherical shape. In order to reach the high spin values of the superdeformed states, more d bosons are needed. This, in turn, increase the energy of the state. Therefore, from both considerations of energy and superdeformation, low n_Δ dominance is reasonable.

IV. SUMMARY

The superdeformed bands of ^{191,193}Hg are studied by coupling single-fermion orbitals with the superdeformed interacting boson model. For each superdeformed band, we include the corresponding dominant fermion orbital suggested by the experimental data. In general, the energy level spectra can be reproduced quite well. The dynamic moments of inertia can be reproduced reasonably well. It was found that in the boson interactions a modified form of angular momentum-angular momentum interaction and the term $n_d\varepsilon_d$ are the most important ones. For the boson-fermion interaction the quadrupole-quadrupole interaction is the most important one and the exchange interaction can be neglected. The calculated values of ε_d which are around 0.1 MeV or smaller are much smaller than those found in normal interacting boson model calculations. Therefore, in the picture of superdeformed interacting boson model, the superdeformed nuclei can be considered as numerous superdeformed bosons interact with a smaller core and among themselves. The small values of ε_d suggest that the energy gaps between the s-boson and d-boson orbitals are small. Except for the cases of structure changes, the general behaviors of the dynamic moments of inertia (J_2) can be reproduced. We would like to mention the following two theory-experiment discrepancies: (i) For those experimental data which show a very quick variation of J_2 versus the change of rotational energy, the calculation can only provide a correct result in the sense of average. The staggering of dynamic moment of inertia observed in some superdeformed bands can not be reproduced. This theory-experiment discrepancy also happens in the superdeformed interacting boson model calculation on even-even Hg isotopes. In order to explain the staggering, apparently a refined model is needed. (ii) For the superdeformed band which shows band crossing (band 1 of ^{193}Hg), it is not possible to reproduce the J_2 values for the whole range of rotational energies. It will be interesting to see whether the experimental data can be reproduced by introducing two or more single-fermion orbitals simultaneously in the calculation on this band. However, this will enlarge the model space and a more radical truncation to the model space is needed to make the calculation feasible. For a calculation which demands very small theory-experiment discrepacies in energy level spacings, this becomes a rather large uncertain factor. Furthermore, this also introduces more interaction parameters in the calculation and the determination of the interaction parameters by the least-squares fittings will be much more cumbersome.

The criterion of stability selects low-energy configurations. This can be achieved by having a small number of d-bosons or a strong boson pairing. However, in our calculation it was found that the boson pairing interaction can be neglected. This is consistent with the picture of superdeformation since the pairing has the tendency to restore the nucleus to a spherical shape. Therefore, we expect a low n_d configuration dominance. The analysis on the energy eigenfunctions indeed reveal this tendency. However, in order to build up the high spins, many d bosons are needed. Therefore, the superdeformed systems tend to make a most economic coupling to build up the high angular momentum. As a result, the d-boson angular momenta tend to align with each other. Furthermore, the dominance of the states with $J=L+j$ also suggests that the single-fermion angular momentum tends to align with the boson total angular momentum.

The success of the superdeformed interacting-boson-fermion model in correlating the main features of the superdeformed bands of ^{191,193}Hg is encouraging. The model has the advantage to incorporate the fermion degrees of freedom with the even-even core in an easy and consistent way. By including more fermion orbitals, it may be used to study the band crossing mechanisms observed in some superdeformed bands. In the mass number region $A=150$, there are also quite numerous superdeformed band data. As compared with the superdeformed bands in the mass region $A=190$, there are more bands with irregular variations in the moments of inertia. We believe that a detailed calculation on the superdeformed band in the mass region $A=150$ will manifest more clearly the advantages and limitations of the model.

[1] A. Arima and F. Iachello, Ann. Phys. (N.Y.) **99**, 253 (1976).
[2] A. Arima and F. Iachello, Ann. Phys. (N.Y.) **111**, 201 (1978).
[3] A. Arima and F. Iachello, Ann. Phys. (N.Y.) **123**, 468 (1979).
[4] A. Arima and F. Iachello, Phys. Rev. C **14**, 761 (1976).
[5] F. Iachello and O. Scholten, Phys. Rev. Lett. **43**, 679 (1979).
[6] R. Bijker and A. E. L. Dieperink, Nucl. Phys. **A379**, 221 (1982).
[7] M. A. Cunningham, Nucl. Phys. **A385**, 204 (1985).
[8] M. A. Cunningham, Nucl. Phys. **A385**, 221 (1985).
[9] H. C. Chiang, S. T. Hsieh, and D. S. Chun, Phys. Rev. C **39**, 2390 (1989).
[10] S. T. Hsieh, H. C. Chiang, and M. M. King Yen, Phys. Rev. C **41**, 2898 (1990).
[11] T. Otsuka and M. Honma, Phys. Lett. B **268**, 305 (1991).
[12] S. Kuyacak, M. Honma, and T. Otsuka, Phys. Rev. C **53**, 2194 (1996).
[13] Y. X. Liu, J. G. Song, H. Z. Sun, and E. G. Zhao, Phys. Rev. C **56**, 1370 (1997).
[14] E. F. Moore, R. V. F. Janssens, K. R. Chasman, I. Ahmad, T. L. Khoo, F. L. H. Wolfs, D. Ye, K. B. Beard, U. Garg, M. W. Drigert, Ph. Benet, Z. W. Grabowski, and J. A. Cizewski, Phys. Rev. Lett. **63**, 360 (1989).
[15] M. P. Carpenter, R. V. F. Janssens, E. F. Moore, I. Ahmad, P. B. Fernandez, T. L. Khoo, F. L. H. Wolfs, D. Ye, K. B. Beard, U. Garg, M. W. Drigert, Ph. Benet, R. Wyss, W. Sutula, W. Nazarewicz, and M. A. Riley, Phys. Lett. B **240**, 44 (1990).
[16] D. M. Cullen, M. A. Riley, A. Alderson, I. Ali, C. W. Beausang, T. Bengtsson, M. A. Bentley, P. Fallon, P. D. Forsyth, F. Hanna, S. M. Mullins, W. Nazarewicz, R. J. Poynter, P. H. Regan, J. W. Roberts, W. Satula, J. F. Sharpey-Schafer, J. Simpson, G. Sletten, P. J. Twin, R. Wadsworth, and R. Wyss, Phys. Rev. Lett. **65**, 1547 (1990).
[17] M. J. Joyce, J. F. Sharpey-Schafer, P. J. Twin, C. W. Beausang, D. M. Cullen, M. A. Riley, R. M. Clark, P. J. Dagnall, I. Deloncle, J. Duprat, P. Fallon, P. D. Forsyth, N. Fortiades, S. J. Gale, B. Gall, F. Hannachi, S. Harissopulos, K. Hauschild, P. M. Jones, C. A. Kalfas, A. Korichi, Y. Le Coz, M. Meyer, E. S. Paul, M. G. Porquet, N. Redon, C. Schuck, J. Simpson, R. Vlastou, and R. Wadsworth, Phys. Rev. Lett. **71**, 2176 (1993).
[18] M. J. Joyce, J. F. Sharpey-Schafer, M. A. Riley, D. M. Cullen, F. Azaiez, C. M. Beausang, R. M. Clark, P. J. Dagnall, I. Deloncle, J. Duprat, P. Fallon, P. D. Forsyth, N. Fortiades, S. J. Gale, B. Gall, F. Hannachi, S. Harissopulos, K. Hauschild, P. M. Jones, C. A. Kalfas, A. Korichi, Y. Le Coz, M. Meyer, E. S. Paul, M. G. Porquet, N. Redon, C. Schuck, J. Simpson, R. Vlastou, R. Wadsworth, and W. Nazarewicz, Phys. Lett. B **340**, 150 (1994).
[19] M. P. Carpenter, R. V. F. Janssens, B. Cederwall, B. Crowell, I. Ahmad, J. A. Becker, M. J. Brinkman, M. A. Deleplanque, R. M. Dimond, P. Fallon, L. P. Farris, U. Garg, D. Gassmann, E. A. Henry, R. G. Henry, J. R. Hughes, T. L. Khoo, T. Lauristsen, I. Y. Lee, A. O. Machiavelli, E. F. Moore, D. Nisius, and F. S. Stephens, Phys. Rev. C **51**, 2400 (1995).
[20] A. Arima and F. Iachello, Annu. Rev. Nucl. Part. Sci. **31**, 75 (1981).
[21] N. Yoshida, H. Sagawa, T. Otsuka, and A. Arima, Phys. Lett. B **256**, 129 (1991).
[22] J. Jerasaki, H. Flocard, P. H. Heenen, and P. Bonche, Phys. Rev. C **55**, 1231 (1997).
[23] H. Z. Sun, M. Zhang, Q. Z. Han, and G. L. Long, J. Phys. A **23**, 1950 (1990).